A Hybrid Approach for Online Joint Detection and Tracking for Multiple Targets

William Ng, Jack Li, Simon Godsill, and Jaco Vermaak
Department of Engineering
University of Cambridge
Emails: {kfn20 ,jfl28, sjg, jv211}@eng.cam.ac.uk

Abstract—In this paper, we present a new approach for online joint detection and tracking for multiple targets. We combine a deterministic clustering algorithm for target detection with a sequential Monte Carlo method for multiple target tracking. The proposed approach continuously monitors the appearance and disappearance of a set of regions of interest for target detection within the surveillance region. No computational effort for target tracking will be expended unless these regions of interest are persistently detected. In addition, we also integrate a very efficient 2-D data assignment algorithm into the sampling method for the data association problem. The proposed approach is applicable to nonlinear and non-Gaussian models for the target dynamics and measurement likelihood. Computer simulations demonstrate that the proposed hybrid approach is robust in performing joint detection and tracking for multiple targets even though the environment is hostile in terms of high clutter density and low target detection probability.

TABLE OF CONTENTS

1 INTRODUCTION
2 DATA MODEL
3 INTRODUCTION TO THE REGIONS OF INTEREST
4 SEQUENTIAL MONTE CARLO METHODS
5 CLUSTERING ALGORITHM
6 $\mathfrak{M}$-BEST 2-D MEASUREMENT-TO-TARGET ASSIGNMENT ALGORITHM
7 COMPUTER SIMULATIONS
8 CONCLUSIONS
9 ACKNOWLEDGEMENTS

1. INTRODUCTION

Multitarget tracking (MTT) [1], [2], [3] that deals with the multitarget state estimation of moving targets may find applications in radar and sonar based tracking of objects, for example. There have been advances in different strategies, including the classical Joint Probabilistic Data Association Filter (JPDAF) [1], [4] and a variety of its derivatives, and the recently popoular sequential Monte Carlo (SMC) methods [5], [6], [7], for tackling the target tracking and data association problems. The former approaches essentially adopt the classical methods like the extended Kalman Filter [8] (EKF) for multitarget state estimation, whose tracking performance is known to be limited by the linearity of the data models. On the contrary, the latter approaches are able to perform well even when the data models are nonlinear and non-Gaussian. However, almost all of these methods assume that the knowledge of the true targets, including when and where they appear and disappear, is given. Accordingly, methods relying on this unrealistic assumption are not practical for real-life applications.

In fact, online joint detection and tracking for multiple targets remains a challenging problem for surveillance systems using one or multiple sensors to monitor the environment. An observation may consist of measurements due to the moving targets and clutter, which is generally considered as false alarms. As a result, prior to being able to track the states of the true targets, one needs to detect how many active targets are present and to identify which measurements should be associated with the targets, if available. Unfortunately, as the number of targets and clutter rate increase, both the target detection and data association problems becomes more difficult and complex, because false alarms from detecting new targets as a result of high clutter density become more frequent and the computation required for data association increases exponentially as the number of detected targets and clutter rate increase. Thus a robust approach for target detection that is capable of detecting the number of true targets while minimising the number of false alarms in the hostile environment, and efficient data association approaches are required.

Recently, the sequential Monte Carlo (SMC) technique [5], [6], [7], otherwise known as Particle Filtering [9], [10], has become a popular framework for target tracking, because it is able to perform well even when the data models are nonlinear and non-Gaussian. Given the latest observations and the past target state information in terms of an estimate of the posterior distribution function, SMC methods that employ sequential importance sampling can recursively update the posterior distribution of the target state optimally through time. The Probability Hypothesis Density (PHD) filter [11], [12], [13], [14], which combines the Finite Set Statistics (FISST), an extension of Bayesian anal-

IEEEAC paper # 1606, Version 1, Update October 27 2004

ysis to incorporate comparisons between different dimensional state-spaces, and the SMC methods, is proposed for joint target detection and estimation. While this approach is theoretically sound, it demands intense computation, with a huge number of particles required to explore different dimensional state-spaces for target detection. Moreover, it is found that the performance of the approach in terms of target detection and estimation is significantly degraded when the environment is hostile – high clutter density and low target detection probability.

In this paper we introduce a hybrid approach to perform online joint detection and tracking for multiple targets. This approach is composed of two parts. The first part is to use a deterministic clustering approach that searches for regions of interest (ROIs) based on the observations and monitors these ROIs for target detection. The second part is to adopt SMC methods to perform multitarget state tracking, based on the sequential importance sampling with the ROIs. The SMC methods use a set of samples, or *particles*, and associated importance weights, which are then propagated through time to give approximations of the posterior distribution function of the targets at subsequent time steps.

The strategy behind the proposed approach is that we use the most efficient and effective method to locate ROIs, and then apply the computationally intensive SMC methods for tracking the persistent events being represented by the ROIs. All particles will share the same dimensions equal to the number of targets obtained from the clustering algorithm. Moreover, the proposed approach does not impose a maximum number of targets to be tracked; the dimension of the multitarget state vector is time-varying, according to the detected number of targets. As a result, the demanding computational effort required in the SMC-based tracking is expended only where necessary.

The innovative clustering algorithm is robust and effective in locating ROIs, even when the environment is hostile. Monitoring the appearance and disappearance of the ROIs enables us to detect the number targets for tracking. As each ROI represents a set of target originating measurements within a short period of time and the surveillance region, it enables us to involve the current observations in sampling the particles, yielding better responses and performance in target tracking, especially when the targets make sudden and sharp turns. Moreover, the ROIs can be used to effectively initialise the target state vectors when new tracks are initiated, when compared to other approaches that attempt to randomly or blindly initialise these new target state vectors within the entire state-space.

In this paper we also propose a new data association method that combines the efficent 2-D data assignment method with sampling methods in the SMC framework. Unlike the best solution approach [15], [16], [17], [18], [19] used for data association for MTT problem, the proposed approach first computes the $\mathfrak{M}$-best feasible solutions [16], [17], [18], [19] and their associated utility using the 2-D assignment method, subject to certain feasibility constraints, and then samples a solution according to a discrete proposal distribution function with support of these $\mathfrak{M}$ points. Not only does this approach provide flexibility in determining the measurement-to-target assignment, it also fits well to the SMC framework.

This paper is organised as follows. Section 2 presents the state-space model and the derivation of the distributions. Section 3 presents the introduction to ROIs and describes how to detect the number of targets using these ROIs. Section 4 describes the derivation of the sequential update of the target posterior distribution and the birth, death, and update moves, respectively. Section 5 presents the clustering algorithm, followed by the data association using the $\mathfrak{M}$-best approach in Section 6. Section 7 presents simulation results. Conclusions are given in Section 8.

Notation: Bold upper case symbols denote matrices, and bold lower case symbols denote vectors. The superscript ^{T} denotes the transpose operation, and the symbol "$\sim$" means "distributed as." The quantity $\pi(\cdot|\cdot)$ denotes a posterior distribution, whereas $q(\cdot|\cdot)$ denotes a proposal distribution function. The quantity $\mathcal{N}(\boldsymbol{\mu}, \boldsymbol{\Sigma})$ indicates a real normal distribution with mean $\boldsymbol{\mu}$ and covariance matrix $\boldsymbol{\Sigma}$. The quantity $\mathcal{U}(a, b)$ indicates a uniform distribution over the interval $[a, b]$, or $\mathcal{U}_V$ indicates a uniform distribution inside the volume V.

2. Data Model

State-Space and Dynamics

In this section, we will provide a brief description of the state-space model for target tracking. Denoting the combined state vector for K_t unknown and time-varying targets by $\boldsymbol{x}_t = [\boldsymbol{x}_{1,t}^T, ..., \boldsymbol{x}_{k,t}^T, ..., \boldsymbol{x}_{K_t,t}^T]^T$, we have the state evolution equation for the kth target $\boldsymbol{x}_{k,t}$, i.e.,

$$\boldsymbol{x}_{k,t} = \boldsymbol{f}_k(\boldsymbol{x}_{k,t-1}) + \boldsymbol{v}_{k,t},\ k \in \{1, ..., K_t\}, \tag{1}$$

where $\boldsymbol{f}_k(\cdot)$, which models the maneuvering of the target, can be a linear or nonlinear function. The noise $\boldsymbol{v}_{k,t}$ is a zero-mean random variable with a fixed and known covariance matrix $\boldsymbol{\Sigma}_v$.

To track the time-varying number of targets K_t, in this paper we opt the approach of having a variable dimenionsal state-space. The number of targets K_t is modelled by the following stochastic relationship at time t

$$K_t = K_{t-1} + \epsilon_{K_t}, \tag{2}$$

where ϵ_{K_t} is a discrete iid random variable such that

$$\begin{aligned} \mathbf{Pr}(\epsilon_{K_t} = -1) &= h_d, \\ \mathbf{Pr}(\epsilon_{K_t} = 0) &= 1 - h_b - h_d, \\ \mathbf{Pr}(\epsilon_{K_t} = 1) &= h_b, \end{aligned} \tag{3}$$

where $h_b, h_d \in \{0, 1\}$, implying that the number of targets can change by no more than one at a given time. In general, we set $h_d = h_b = h/2$, where $h \in \{0, 1\}$, but when $K_{t-1} = 0$, we set $h_d = 0$ and $h_b = h$. Accordingly, we may express the following joint dynamics for state and number of targets

$$p(\boldsymbol{x}_t, K_t|\boldsymbol{x}_{t-1}, K_{t-1}) = p(\boldsymbol{x}_t|\boldsymbol{x}_{t-1}, K_t, K_{t-1})\times p(K_t|K_{t-1}), \tag{4}$$

where $p(\boldsymbol{x}_t|\boldsymbol{x}_{t-1}, K_t, K_{t-1})$ is the dynamic prior function for the combined state vector, and $p(K_t|K_{t-1})$ is the prior distribution of K_t according to (2) and (3). It is assumed that all targets are moving independently according to Markovian dynamics [1], [20], and that all targets share the same dynamic model. Then we have

$$p(\boldsymbol{x}_t|\boldsymbol{x}_{t-1}, K_t, K_{t-1}) = \begin{cases} p_0(\boldsymbol{x}_{K_t,t}) \prod_{k=1}^{K_{t-1}} p(\boldsymbol{x}_{k,t}|\boldsymbol{x}_{k,t-1}), & \text{if } K_t = K_{t-1}+1, \\ \prod_{k=1}^{K_t} p(\boldsymbol{x}_{k,t}|\boldsymbol{x}_{k,t-1}), & \text{if } K_t = K_{t-1}, \\ \prod_{k=1,k\neq k^*}^{K_t} p(\boldsymbol{x}_{k,t}|\boldsymbol{x}_{k,t-1}), & \text{if } K_t = K_{t-1}-1, \end{cases} \tag{5}$$

where $p_0(\boldsymbol{x}_{K_t,t})$ is the distribution function for a new target detected at t and k^* is a target that has disappeared at t.

Observation Model and Likelihood

We consider a single observer, located at a fixed and known position (x_o, y_o), scanning within the surveillance region $\mathcal{R}_V$, but note that the models and algorithms could be extended for multiple observers. At any particular time, the sensor receives an observation vector $\boldsymbol{y}_t = [\boldsymbol{y}_{1,t}^T, ..., \boldsymbol{y}_{m,t}^T, ..., \boldsymbol{y}_{M_t,t}^T]^T$, where the number of measurements M_t varies with time. The measurements are assumed independent of each other and may originate from true targets or from clutter. Furthermore, we assume that each of the true targets can generate at most one measurement at a given time but may go undetected. As in [20], if the mth measurement of $\boldsymbol{y}_t$ is due to the kth target, it follows that

$$\boldsymbol{y}_{m,t} = \boldsymbol{g}_m(\boldsymbol{x}_{k,t}) + \boldsymbol{w}_{m,t}, \tag{6}$$

where $\boldsymbol{g}_m(\cdot)$ may be a nonlinear function and $\boldsymbol{w}_{m,t}$ is a zero-mean random variable with covariance $\boldsymbol{\Sigma}_w$. Accordingly, we may express the likelihood for a measurement due to a target as

$$p(\boldsymbol{y}_{m,t}|\boldsymbol{x}_{k,t}),\ m \in \{1, ..., M_t\}. \tag{7}$$

If, on the contrary, the measurement is due to clutter, we will assume it to be a uniform distribution over the surveillance region, i.e.,

$$p(\boldsymbol{y}_{m,t}) = \mathcal{U}_{\mathcal{R}_V}(\boldsymbol{y}_{m,t}),\ m \in \{1, ..., M_t\}, \tag{8}$$

where V is the volume of the surveillance region R_V.

Since measurements do not only arise from the targets but also from spurious objects, such as clutter, we need to properly deal with the data association problem, i.e., measurment-to-target assignment, prior to target tracking. Following the framework in [15], [21], [22], we adopt the assumption that $\lambda_t = (\boldsymbol{\alpha}_t, N_{C_t}, N_{D_t})$, a *measurement-to-target association* hypothesis, is a stochastic variable which is dependent on the current targets' state and observations. The association vector $\boldsymbol{\alpha}_t$ is defined as

$$\boldsymbol{\alpha}_t = [\alpha_{1,t}, ..., \alpha_{m,t}, ..., \alpha_{M_t,t}]^T, \tag{9}$$

with elements

$$\alpha_{m,t} = \begin{cases} k \in \{1, ..., K_t\}, & \text{if } \boldsymbol{y}_{m,t} \text{ originates from target } k, \\ 0, & \text{otherwise,} \end{cases} \tag{10}$$

and N_{C_t} and N_{D_t} are the number of clutter measurements and detected targets, respectively. More details about the derivation of the posterior distribution function and the prior functions of the parameters will be given later.

Given the association hypothesis the likelihood for the observation $\boldsymbol{y}_t$ becomes [21], [23]

$$\begin{aligned} p(\boldsymbol{y}_t|\boldsymbol{x}_t, K_t, \lambda_t) &= \prod_{m=1}^{M_t} p(\boldsymbol{y}_{m,t}|\boldsymbol{x}_t, K_t, \lambda_t), \\ &= V^{-N_{C_t}} \prod_{l\in\mathcal{I}_D} p(\boldsymbol{y}_{l,t}|\boldsymbol{x}_{\alpha_{l,t},t}), \end{aligned} \tag{11}$$

where $\mathcal{I}_D$ is the set of observation indices corresponding to the N_{D_t} detected targets.

Posterior Distribution Function

In our problem, the variables of interest are $\boldsymbol{\theta}_{1:t} \triangleq \{\boldsymbol{x}_{1:t}, K_{1:t}, \lambda_{1:t}\}$, where the notation $(\cdot)_{1:t}$ indicates all the elements from time 1 to time t. The posterior distribution for these variables, given the observations $\boldsymbol{y}_{1:t}$, may be obtained from Bayes' theorem [24] as

$$p(\boldsymbol{\theta}_{1:t}|\boldsymbol{y}_{1:t}) \propto \prod_{l=1}^{t} p(\boldsymbol{y}_l|\boldsymbol{\theta}_l)\, p(\boldsymbol{\theta}_l|\boldsymbol{\theta}_{l-1}), \tag{12}$$

where $p(\boldsymbol{y}_l|\boldsymbol{\theta}_l) = p(\boldsymbol{y}_l|\boldsymbol{x}_l, K_l, \lambda_l)$ is the likelihood function from (11). The quantity $p(\boldsymbol{\theta}_l|\boldsymbol{\theta}_{l-1})$ is a product of prior functions, given by

$$p(\boldsymbol{\theta}_l|\boldsymbol{\theta}_{l-1}) = p(\boldsymbol{x}_l|\boldsymbol{x}_{l-1}, K_l, K_{l-1})\, p(\lambda_l|\boldsymbol{x}_l, K_l) \times p(K_l|K_{l-1}), \tag{13}$$

where the first term in (13) is the dynamic prior in (4) for all the targets, whereas the second term is the prior for the association hypothesis, and we assume it to take the same form as in [21]. For $t = 1$, we denote the initial distributions for the number of targets and the target state by $p(K_1|K_0) \triangleq p(K_1)$, and $p(\boldsymbol{x}_1|\boldsymbol{x}_0, K_1, K_0) \triangleq p(\boldsymbol{x}_1)$, respectively.

Association Prior

Here we follow the definitions of the association hypothesis λ_t in [21] and adopt it as a stochastic variable which is dependent on the current targets' state and observations, i.e., $\lambda_t = (\boldsymbol{\alpha}_t, N_{C_t}, N_{D_t})$. It is assumed that the association hypothesis has the following hierarchical structure [21], [25]

$$p(\lambda_t|K_t) = p(\boldsymbol{\alpha}_t|K_t, N_{C_t}, N_{D_t})\, p(N_{C_t})\, p(N_{D_t}|K_t), \tag{14}$$

where

$$p(\boldsymbol{\alpha}_t|K_t, N_{C_t}, N_{D_t}) = N_{\lambda_t}^{-1}(K_t, N_{C_t}, N_{D_t}), \tag{15}$$

$$p(N_{C_t}) = (\Lambda_C)^{N_{C_t}} \exp(-\Lambda_C)/N_{C_t}!, \tag{16}$$

$$p(N_{D_t}|K_t) = \binom{K_t}{N_{D_t}} P_D^{N_{D_t}} (1 - P_D)^{K_t - N_{D_t}}. \tag{17}$$

The prior in (15) represents the number of valid hypothesis, given by

$$N_{\lambda_t}(K_t, N_{C_t}, N_{D_t}) = \binom{M_t}{N_{D_t}} \frac{K_t!}{(K_t - N_{D_t})!}. \tag{18}$$

It is assumed that the number of clutter N_{C_t} follows a Poisson distribution in (16) with the expected value Λ_C, which is assumed fixed and known. Finally, the binomial prior in (17) represents the number detected target originating measurements out of the number of targets K_t with a fixed and known P_D, target detection probability, shared by all targets.

3. Introduction to the Regions of Interest

Denote a buffer of observations by $\boldsymbol{\mathcal{Y}}_t = \{\boldsymbol{y}_{t'}, t' \in \{t - \tau, t\}\}$, where τ is the width of the buffer, and a set of regions of interest (ROIs), by $\boldsymbol{\mathcal{S}}_t = \{\mathcal{S}_t^{(j)}, j = 1, ..., J_t\}$, where J_t is the number of ROIs found at t within $\boldsymbol{\mathcal{Y}}_t$. Each region $\mathcal{S}_t^{(j)}$ is constructed from a cluster of measurements received in $\boldsymbol{\mathcal{Y}}_t$, and is a subspace of the surveillance region $\mathcal{R}_V$, i.e., $\mathcal{S}_t^{(j)} \subset \mathcal{R}_V, j \in \{1, ..., J_t\}$.

Within the buffer $\boldsymbol{\mathcal{Y}}_t$, some events may have happened and may be caused by the movement of the true target(s) and/or the presence of spurious objects, such as clutter, if they do exist. As a result, we may express $J_t = K_t^c + K_t$, where K_t^c is the number of clutter regions, and K_t is the number of true targets comprising the active targets that have been tracked and the new targets that may have just appeared, respectively. Denote the number of true targets that are active and have been tracked by $K_t^{a'}$ and the number of true targets that have not been detected until t by K_t^b, respectively. For those $K_t^{a'}$ active tracks, two types of targets are present. One is active and is not likely to vanish within any detected ROIs, whereas the other type is also active but may vanish within some of the detected ROIs, as these tracks have not been associated with any measurement over a certain scans. Let K_t^a (K_t^d) be the number of targets that are active, have been tracked, and have (not) been associated with at least one measurement in $\boldsymbol{\mathcal{Y}}_t$. Accordingly, we may rewrite the number of true targets K_t for multitarget tracking as

$$K_t = J_t - K_t^c = K_t^a + K_t^b - K_t^c - K_t^d. \tag{19}$$

Therefore, to detect the number of true targets K_t online and hence estimate the multitarget states, we may first detect the ROIs, given the buffer of observations $\boldsymbol{\mathcal{Y}}_t$, and then *classify* them into one of the following classes: active tracks, new tracks, vanishing tracks, and false alarms.

History of ROIs

As described earlier, each ROI is essentially composed of a cluster of measurements, so we may express a region $\mathcal{S}_t^{(j)}$ in terms of a set of time and observation indices in $\boldsymbol{\mathcal{Y}}_t$ that are grouped to construct the region as follows

$$\mathcal{S}_t^{(j)} = \{\boldsymbol{t}^{(j)}, \boldsymbol{m}^{(j)}\},\ \boldsymbol{t}^{(j)}, \boldsymbol{m}^{(j)} \in \mathcal{R}^{P_t^{(j)} \times 1}, \tag{20}$$

where $P_t^{(j)}$ is the number of measurements or number of pairs included in the region. The lth pair of $\boldsymbol{t}^{(j)}$ and $\boldsymbol{m}^{(j)}$, i.e., $(t_l^{(j)}, m_l^{(j)})$, indicates that the $m_l^{(j)}$th measurement of $\boldsymbol{y}_{t_l^{(j)}}$ is part of $\mathcal{S}_t^{(j)}$ with $t_l^{(j)} \in \{t - \tau, t\}$ and $m_l^{(j)} \in \{1, ..., M_{t_l^{(j)}}\}$.

Given another region $\mathcal{S}_{t'}^{(j')}$, the regions $\mathcal{S}_t^{(j)}$ and $\mathcal{S}_{t'}^{(j')}$ with $j \neq j'$ and $t \neq t'$, are said to have a *relationship* if *their respective subsets of time and observation indices are identical.* Let $\tilde{\mathcal{S}}_t^{(j)}$ be a subset of $\mathcal{S}_t^{(j)}$, i.e., $\tilde{\mathcal{S}}_t^{(j)} \subset \mathcal{S}_t^{(j)}$, where

$$\tilde{\mathcal{S}}_t^{(j)} = \{\tilde{\boldsymbol{t}}^{(j)}, \tilde{\boldsymbol{m}}^{(j)}\},\ \tilde{\boldsymbol{t}}^{(j)} \subset \boldsymbol{t}^{(j)}, \tilde{\boldsymbol{m}}^{(j)} \subset \boldsymbol{m}^{(j)}. \tag{21}$$

Therefore, if the subsets $\tilde{\mathcal{S}}_t^{(j)}$ and $\tilde{\mathcal{S}}_{t'}^{(j')}$ are identical, the regions $\mathcal{S}_t^{(j)}$ and $\mathcal{S}_{t'}^{(j')}$ are related, and the region found earlier is a predecessor of the other one found later. In other words, given a region it is always possible to trace the history of the region – its predecessors and successors. This information is useful to determine whether an event being represented by a set of related regions over time is persistent in order to take appropriate actions, such as *the birth* or *death* move (see Section 4). For example, an event due to a true target may be detected almost every time when a new observation arrives, provided the probability of target detection is moderate. Therefore, the number of regions representing this event is certainly growing with time, because the event is persistent. As a result, new track initiation may proceed to start tracking the new target. On the other hand, if an event originates from clutter, it is expected that this event does not last long where only a very small number of regions represents the event; the event can be ignored.

Classification of ROIs

To identify the regions originating from false alarms or clutter from $\boldsymbol{\mathcal{S}}_t$ is relatively simple and effective, given the distinct characteristic of clutter. As described in (8), the distribution of clutter measurements is completely random and it is not likely to form any *pattern* or a cluster of measurements in the vicinity of each other within τ scans. The clustering algorithm to be given in Section 5 describes in detail how to detect and reduce the false alarms in $\boldsymbol{\mathcal{S}}_t$. In case when a clutter region cannot be filtered out by the clustering algorithm, it is possible to distinguish between this false alarm and other target regions, since the life span of the event represented by this false alarm region is very short when compared with that of a true target.

In order to decide whether a given region belongs to an existing active track or a new track, an association between the ROIs and the active tracks is needed. Let $\boldsymbol{\gamma}_t = [\gamma_{1,t}, ..., \gamma_{k,t}, ..., \gamma_{K_t,t}]^T$ be a *track-to-region* association vector, where

$$\gamma_{k,t} = \begin{cases} j \neq 0, & \text{if track } k \text{ can be associated with } \mathcal{S}_t^{(j)}, \\ 0, & \text{otherwise}, \end{cases} \tag{22}$$

and let $\boldsymbol{\beta}_t = [\beta_{1,t}, ..., \beta_{j,t}, ..., \beta_{J_t,t}]^T$ be a *region-to-track* association vector, where

$$\beta_{j,t} = \begin{cases} k \neq 0, & \text{if } \mathcal{S}_t^{(j)} \text{ can be associated with track } k, \\ 0, & \text{otherwise}, \end{cases} \tag{23}$$

with $j \in \{1, ..., J_t\}$ and $k \in \{1, ..., K_t\}$. From (23), we can determine the possible number of new tracks for initiation, K_t^b, i.e., the number of zero elements of $\boldsymbol{\beta}_t$ as these regions with $\beta_{j,t} = 0$ cannot find an association with the existing active tracks. Let $\mathcal{I}_b$ be a set of region indices that the corresponding regions cannot be associated with the existing active tracks, i.e., $\mathcal{I}_b = \{j : \beta_{j,t} = 0, \ j = 1, ..., J_t\}$. Following the steps in the birth move (see Section 4), these K_t^b new tracks will be created and initialised properly using the ROIs $\mathcal{S}_t^{(j)}$, $j \in \mathcal{I}_b$. To avoid prematurely initiating a new track from an unassociated region that may originate from a false alarm, it is more appropriate to examine the history of the unassociated region as described in Section 3 and to ensure that it is persistent enough for initiating a new track. For example, a region $\mathcal{S}_t^{(j)}$ will be used to initiate a new track if 1) none of its predecessors has been associated with any active track, and 2) the time difference between the current time and the time that its first predecessor was found is at least τ_b, implying that an event being detected by this sequence of regions is persistent and the birth move may proceed to initiate a new track for tracking this event.

On the other hand, the vector $\boldsymbol{\gamma}_t$ can be used to determine which active tracks can be updated using SMC methods and which active tracks may vanish with which the death move (see Section 4) is proceeded. The number of active and associated tracks K_t^a is given by the number of nonzero elements of $\boldsymbol{\gamma}_t$ in (22). Let $\mathcal{I}_a$ be a set of region indices that the corresponding regions can be associated with the existing active tracks, i.e., $\mathcal{I}_a = \{j : \gamma_{k,t} = j, \ j = 1, ..., J_t, \ k = 1, ..., K_t\}$. The *update move* (see Section 4) will be performed with the ROIs $\mathcal{S}_t^{(j)}$, $j \in \mathcal{I}_a$ on these K_t^a tracks.

Those tracks with $\gamma_{k,t} = 0$ may imply two scenarios. One scenario is that the targets that have been estimated by these active tracks have vanished, and hence no longer generate new measurements that can be associated with these tracks. Thus these tracks will be removed from the tracker as a result. The other scenario is that these track may encounter a data loss in a few scans in which not only can no regions be formed when no measurements have been received during this period, but these tracks also cannot be associated with any measurements. Therefore, it is necessary to avoid prematurely removing a track with $\gamma_{k,t} = 0$, based solely on the ROIs at one particular time. Instead, a track can only be removed from the tracker if the track cannot be associated with any ROI or measurement over a period of time, say τ_d. Let t_k^a be the time index when the kth track can be associated with a ROI. Therefore, if $t - t_k^a \geq \tau_d$, then the death move will be proceeded to properly remove the kth track from the tracker. Otherwise, it should remain intact.

In short, by continuously monitor the appearance and disappearance of a set of ROIs $\boldsymbol{\mathcal{S}}_t$ over time, we are able to detect the number of targets for initiation (the birth move), for removal (the death move), and for estimation (the update move), with the use of the association vectors $\boldsymbol{\gamma}_t$ and $\boldsymbol{\beta}_t$ in (22) and (23), respectively.

Track-to-region and region-to-track association

One key to successfully performing target detection is to obtain the association vectors $\boldsymbol{\gamma}_t$ and $\boldsymbol{\beta}_t$ in (22) and (23), respectively. Assuming that a track estimating a true target at $t-1$ can be associated with a measurement of $\boldsymbol{y}_{t-1}$, we may associate the track with one of the regions in $\boldsymbol{\mathcal{S}}_t$ in order to determine the vector $\boldsymbol{\gamma}_t$. To do so, we need to involve the data association vector $\boldsymbol{\alpha}_{t-1}$, whose nonzero elements $\alpha_{m,t-1} = k$ indicates which measurement is associated with which track. If the measurement $\boldsymbol{y}_{m,t-1}$ was associated with the kth track, and if this pair of indices $(t-1, m_{t-1})$ is included in the region $\mathcal{S}_t^{(j)}$, defined in (20), then the kth track is associated with the region $\mathcal{S}_t^{(j)}$, i.e., $\gamma_{j,t} = k$ and $\beta_{k,t} = j$. In general, the kth track is associated with the jth region if the measurement that the track last took for data association is included in the region $\mathcal{S}_t^{(j)}$.

4. SEQUENTIAL MONTE CARLO METHODS

Sequential Monte Carlo (SMC) methods [5], [6], [7], otherwise known as Particle Filters [9], [10], have gained popularity in recent years as a numerical approximation strategy for recursive estimation for complex models. This is due to their simplicity, flexibility, ease of implementation, and modelling success over a wide range of challenging applications.

In this section, we briefly describe the particle filter tracking framework for our state-space model. In the context of tracking, we are interested in the posterior distribution $p(\boldsymbol{\theta}_t|\boldsymbol{y}_{1:t})$, where $\boldsymbol{\theta}_t = \{\boldsymbol{x}_t, K_t, \lambda_t\}$, which can be recursively obtained according to the Bayesian Sequential Estimation framework, as follows

$$p(\boldsymbol{\theta}_t|\boldsymbol{y}_{1:t}) \propto p(\boldsymbol{y}_t|\boldsymbol{\theta}_t)\times \int p(\boldsymbol{\theta}_t|\boldsymbol{\theta}_{t-1})\, p(\boldsymbol{\theta}_{t-1}|\boldsymbol{y}_{1:t-1})\, d\boldsymbol{\theta}_{t-1}, \tag{24}$$

where $p(\boldsymbol{\theta}_{t-1}|\boldsymbol{y}_{1:t-1})$ is the posterior distribution at $t-1$. We may also expand the first term in the integral in (24) in the same spirit to (13). The recursion in (24) is initialised with some distribution, say $p(\boldsymbol{\theta}_0) = p(\boldsymbol{x}_0, K_0, \lambda_0)$. Once the sequence of filtering distributions is known, statistical inferences, like expectation, maximum *a posteriori* (MAP) estimates, and minimum mean square error (MMSE), etc., can be computed.

Sequential Importance Sampling

The basic idea behind particle filters is very simple. Given a set of N particles $\boldsymbol{\theta}_{t-1}^{(i)} = \{\boldsymbol{x}_{t-1}^{(i)}, K_{t-1}^{(i)}, \lambda_{t-1}^{(i)}\}_{i=1}^{N}$ with the associated importance weights $\{w_{t-1}^{(i)}\}_{i=1}^{N}$ that is approximately distributed according to $p(\boldsymbol{\theta}_{t-1}|\boldsymbol{y}_{1:t-1})$, we would like to generate a set of new particles $\{\boldsymbol{\theta}_t^{(i)}\}_{i=1}^{N}$ from an appropriately selected proposal function, i.e.,

$$\boldsymbol{\theta}_t^{(i)} \sim q(\boldsymbol{\theta}_t|\boldsymbol{\theta}_{t-1}^{(i)}, \boldsymbol{\mathcal{Y}}_t), \quad i = \{1, ..., N\}, \tag{25}$$

where $\boldsymbol{\mathcal{Y}}_t$ is defined in Section 3. As a result, the associated weights $w_t^{(i)}$ may be recursively updated as follows

$$w_t^{(i)} \propto w_{t-1}^{(i)} \frac{p(\boldsymbol{y}_t|\boldsymbol{\theta}_t^{(i)})\, p(\boldsymbol{\theta}_t^{(i)}|\boldsymbol{\theta}_{t-1}^{(i)})}{q(\boldsymbol{\theta}_t|\boldsymbol{\theta}_{t-1}^{(i)}, \boldsymbol{\mathcal{Y}}_t)}, \quad \sum_{i=1}^{N} w_t^{(i)} = 1. \tag{26}$$

The particles $\{\boldsymbol{\theta}_t^{(i)}\}_{i=1}^{N}$ with the associated importance weights $\{w_t^{(i)}\}_{i=1}^{N}$ are then approximately distributed according to $p(\boldsymbol{\theta}_t|\boldsymbol{y}_{1:t})$. As the particle filters operate, only a few particles contribute significant importance weights in (26), leading to the degeneracy problem [5], [6]. To avoid this problem, one needs to resample the particles according to the importance weights. That is, those particles with more significant weights will be selected more frequently than those with less significant weights. More detailed discussion of degeneracy and resampling may be found in [6].

Importance Sampling Function

The key to generating a set of weighted particles to suitably approximate the posterior distribution function in (24) is the selection of the proposal importance sampling function $q(\boldsymbol{\theta}_t|\boldsymbol{\theta}_{t-1}^{(i)}, \boldsymbol{\mathcal{Y}}_t)$ [5]. In this paper, the proposal function is given as follows

$$q(\boldsymbol{\theta}_t|\boldsymbol{\theta}_{t-1}^{(i)}, \boldsymbol{\mathcal{Y}}_t) = q(\lambda_t|\boldsymbol{x}_t^{(i)}, K_t^{(i)}, \boldsymbol{y}_t)\times q(\boldsymbol{x}_t|\boldsymbol{x}_{t-1}^{(i)}, K_t^{(i)}, K_{t-1}^{(i)}, \boldsymbol{\mathcal{Y}}_t)\, q(K_t|K_{t-1}^{(i)}, \boldsymbol{\mathcal{Y}}_t), \tag{27}$$

where the first term on the right-hand side is the proposal function for λ_t, the second term is known as the importance sampling function for $\boldsymbol{x}_t$, and the last term is the proposal function for K_t. It is assumed that the association hypothesis λ_t only depends on the information at t, and hence there is only a weak temporal dependence between the association hypotheses λ_t and λ_{t-1}.

As described in Section 3, by monitoring the appearance and disappearance of the ROIs $\boldsymbol{\mathcal{S}}_t \subseteq \boldsymbol{\mathcal{Y}}_t$, one may deterministically obtain an estimate of the number of targets, say $K_t = K^*$, with probability one. Since all particles are to share the same value of K_t, the proposal function $q(K_t|K_{t-1}^{(i)}, \boldsymbol{\mathcal{Y}}_t)$ is not applicable in this paper. From this point onward, as we intend to remain the notation $K_t^{(i)}$ intact in the the subsequent development, the particles $\{K_t^{(i)}\}_{i=1}^{N}$ will share the value that is determined according to Section 3.

In practice, the importance sampling function for $\boldsymbol{x}_t$ in (27) may be hard to design even though only the current observation $\boldsymbol{y}_t \subset \boldsymbol{\mathcal{Y}}_t$ is used as it requires the knowledge of which measurements in $\boldsymbol{y}_t$ are associated with each target. Here we propose to use an importance function that combines the dynamic prior and the current ROIs to generate representative particles for multitarget tracking as follows

$$q(\boldsymbol{x}_t|\boldsymbol{x}_{t-1}^{(i)}, K_t^{(i)}, K_{t-1}^{(i)}, \boldsymbol{\mathcal{Y}}_t) = \mu\, p(\boldsymbol{x}_t|\boldsymbol{x}_{t-1}^{(i)}, K_t^{(i)}, K_{t-1}^{(i)}) + (1-\mu)\, q(\boldsymbol{x}_t|\boldsymbol{x}_{t-1}^{(i)}, K_t^{(i)}, K_{t-1}^{(i)}, \boldsymbol{\mathcal{S}}_t), \tag{28}$$

where $0 \leq \mu \leq 1$. The function $q(\boldsymbol{x}_t|\boldsymbol{x}_{t-1}^{(i)}, K_t^{(i)}, K_{t-1}^{(i)}, \boldsymbol{\mathcal{S}}_t)$ is referred to as the *data-dependent* importance sampling function for the combined state vector $\boldsymbol{x}_t$, as the set $\boldsymbol{\mathcal{S}}_t \subseteq \boldsymbol{\mathcal{Y}}_t$ contains the information about the current observation. If $\mu = 1$, the importance sampling function is reduced back to the dynamic prior. If $\mu = 0$, all particles are generated from the data-dependent importance function. Accordingly, we may sample $\boldsymbol{x}_{k,t}^{(i)}$ as follows

$$\boldsymbol{x}_{k,t}^{(i)} \sim \begin{cases} q_D(\boldsymbol{x}_{k,t}|\boldsymbol{x}_{k,t-1}^{(i)}), & k \notin \mathcal{K}_{\mathcal{S}_t}, \\ q_{DS}(\boldsymbol{x}_{k,t}|\boldsymbol{x}_{k,t-1}^{(i)}, \mathcal{S}_t^{(j)}), & k \in \mathcal{K}_{\mathcal{S}_t}, \end{cases} \tag{29}$$

where $k \in \mathcal{K}_{\mathcal{S}_t}$ are those tracks with $\gamma_{k,t} = j$ and $j \in \mathcal{I}_a$, and $q_D(\cdot)$ and $q_{DS}(\cdot)$ are the proposal functions for $\boldsymbol{x}_{k,t}$ without and with an associated ROI $\mathcal{S}_t^{(j)}$, given as follows, respectively,

$$q_D(\boldsymbol{x}_{k,t}|\boldsymbol{x}_{k,t-1}^{(i)}) = p(\boldsymbol{x}_{k,t}|\boldsymbol{x}_{k,t-1}^{(i)}), \tag{30}$$

$$q_{DS}(\boldsymbol{x}_{k,t}|\boldsymbol{x}_{k,t-1}^{(i)}, \mathcal{S}_t^{(j)}) = \mu\, p(\boldsymbol{x}_{k,t}|\boldsymbol{x}_{k,t-1}^{(i)}) + (1-\mu)\, q(\boldsymbol{x}_{k,t}|\boldsymbol{x}_{k,t-1}^{(i)}, \mathcal{S}_t^{(j)}). \tag{31}$$

Once the set of state particles $\{\boldsymbol{x}_t^{(i)}\}_{i=1}^{N}$ is obtained according to (29), we may obtain the association hypothesis particles $\{\lambda_t^{(i)}\}_{i=1}^N$, according to

$$q(\lambda_t|\boldsymbol{x}_t^{(i)}, \boldsymbol{y}_t) = q(\boldsymbol{\alpha}_t|\boldsymbol{x}_t^{(i)}, \boldsymbol{y}_t). \tag{32}$$

Here we propose to first compute $\mathfrak{M}_t^{(i)}$ feasible solutions in the context of 2-D data assignment problem (see Section 6) and then *sample* an association vector $\boldsymbol{\alpha}_t^{(i)}$, according to a discrete proposal function with support of these $\mathfrak{M}_t^{(i)}$ solutions. That is,

$$\boldsymbol{\alpha}_t^{(i)} \sim q(\boldsymbol{\alpha}_t|\boldsymbol{x}_t^{(i)}, \boldsymbol{y}_t) \propto \sum_{l=1}^{\mathfrak{M}_t^{(i)}} u(\boldsymbol{\alpha}_t^l)\, \delta(\boldsymbol{\alpha}_t - \boldsymbol{\alpha}_t^l), \tag{33}$$

where $u(\boldsymbol{\alpha}_t^l)$ is the probability to obtain the lth measurement-to-target assignment vector, and $\sum_{l=1}^{\mathfrak{M}_t^{(i)}} u(\boldsymbol{\alpha}_t^l) = 1$. Please note the difference in the notation between a particle $\boldsymbol{\alpha}_t^{(i)}$ and a feasible solution $\boldsymbol{\alpha}_t^l$. The former is a *sample* obtained from (33), whereas the latter is a *deterministic solution* obtained from the 2-D assignment algorithm. More details about the 2-D assignment method to obtain the $\mathfrak{M}$-best feasible solutions are given in Section 6.

Given the set of particles $\{\boldsymbol{\theta}_t^{(i)}\}_{i=1}^N = \{\boldsymbol{x}_t^{(i)}, K_t^{(i)}, \lambda_t^{(i)}\}_{i=1}^N$, with $\lambda_t^{(i)} = (\boldsymbol{\alpha}_t^{(i)}, u(\boldsymbol{\alpha}_t^{(i)}), N_{C_t}^{(i)}, N_{D_t}^{(i)})$, where $N_{C_t}^{(i)}$ is the number of zeros in $\boldsymbol{\alpha}_t^{(i)}$ and $N_{D_t}^{(i)} = M_t - N_{C_t}^{(i)}$, the importance weight update equation in (26) for $i \in \{1, ..., N\}$ may be rewritten as

$$w_t^{(i)} \propto w_{t-1}^{(i)} \frac{p(\boldsymbol{y}_t|\boldsymbol{x}_t^{(i)}, K_t^{(i)}, \lambda_t^{(i)})\, p(\lambda_t^{(i)}|\boldsymbol{x}_t^{(i)}, K_t^{(i)})}{u(\boldsymbol{\alpha}_t^{(i)})\, \tilde{q}(\boldsymbol{x}_t^{(i)}|\boldsymbol{x}_{t-1}^{(i)}, K_t^{(i)}, K_{t-1}^{(i)}, \boldsymbol{y}_t)}, \tag{34}$$

where, from (28),

$$\tilde{q}(\boldsymbol{x}_t|\boldsymbol{x}_{t-1}^{(i)}, K_t^{(i)}, K_{t-1}^{(i)}, \boldsymbol{y}_t) = \frac{q(\boldsymbol{x}_t|\boldsymbol{x}_{t-1}^{(i)}, K_t^{(i)}, K_{t-1}^{(i)}, \boldsymbol{y}_t)}{p(\boldsymbol{x}_t|\boldsymbol{x}_{t-1}^{(i)}, K_t^{(i)}, K_{t-1}^{(i)})},$$
$$= \prod_{k \in \mathcal{K}_{S_t}, j \in \mathcal{I}_a} \left\{ \mu + (1-\mu) \frac{q(\boldsymbol{x}_{k,t}|\boldsymbol{x}_{k,t-1}^{(i)}, \mathcal{S}_t^{(j)})}{p(\boldsymbol{x}_{k,t}|\boldsymbol{x}_{k,t-1}^{(i)})} \right\}. \tag{35}$$

Birth and Death Moves

Assuming that there are K_t^b ROIs that cannot be associated with any existing track, we would like to initiate a new track at a given time from one of these regions instead of initiating K_t^b tracks simutaneously so as to fit the birth move with the assumed model of K_t in (2) and (3).

Given an unassociated region $\mathcal{S}_t^{(l)}$, $l = 1, ..., K_t^b$, we will not initiate a new track for this region until object o_l being represented by a set of regions, including $\mathcal{S}_t^{(l)}$ and its predecessors, is persistent. Let $p_b^{o_l}$ be a measure of persistence of object o_l that is being detected by a sequence of regions, including $\mathcal{S}_t^{(l)}$, as follows

$$p_b^{o_l} = \frac{t - t_0^{o_l}}{\tau_b}, \; l = 1, ..., K_t^b, \tag{36}$$

with $t_0^{o_l}$ being the time at which object o_l being represented by the region $\mathcal{S}_t^{(l)}$ is first detected and τ_b being the threshold described in Section 3. The closer the value of $p_b^{o_l}$ to 1, the higher is the certainty that the birth move should be executed to initiate a new track to track the object. Accordingly, we may select region j for new track initiation if $p_b^{o_j} \geq 1$, $j \in \{1, ..., K_t^b\}$, yielding $K_t = K_{t-1} + 1$ after the execution of the birth move. The schema for the birth move is summarised as follows.

Birth Move

1. Assume that K_t^b objects are found and the ROIs representing these objects are unassociated with the existing tracks. We first compute the set of persistence measures $p_b^{o_l}$ in (36) for $l \in \{1, ..., K_t^b\}$, and execute new track initiation as follows
 - If $p_b^{o_j} \geq 1$, $j \in \{1, ..., K_t^b\}$, then for $i \in \{1, ..., N\}$,
 – Sample the multitarget state vector, given $\boldsymbol{x}_{t-1}^{(i)}$ and $\boldsymbol{\mathcal{Y}}_t$ for the existing $K_t^{(i)} = K_{t-1}^{(i)}$ tracks, according to (35), as follows

$$\boldsymbol{x}_t' \sim q(\boldsymbol{x}_t'|\boldsymbol{x}_{t-1}^{(i)}, K_t^{(i)}, K_{t-1}^{(i)}, \boldsymbol{\mathcal{Y}}_t),$$

where the particles $\boldsymbol{x}_t^{\prime(i)}$ are drawn for the existing $K_{t-1}^{(i)}$ tracks.
 – Initialise the particles of the new track with $\mathcal{S}_t^{(j)}$, according to the procedure in Section 5 as follows

$$\tilde{\boldsymbol{x}}_t^{(i)} \sim q(\tilde{\boldsymbol{x}}_t|\mathcal{S}_t^{(j)}).$$

 – Append the two sets of particles to the combined state vector $\boldsymbol{x}_t^{(i)}$ as follows

$$\boldsymbol{x}_t^{(i)} = [\boldsymbol{x}_t^{\prime(i)^T} \,|\, \tilde{\boldsymbol{x}}_t^{(i)^T}]^T.$$

 – Increment the number of targets by one, i.e., $K_t^{(i)} = K_{t-1}^{(i)} + 1$.
 - else, goto Step 2
2. Perform target state estimation with the updated particles $\{\boldsymbol{x}_t^{(i)}, K_t^{(i)}\}_{i=1}^N$ using the update move in Section 4.

When an existing track cannot be associated with a region at a given time, the object being tracked by the tracker may have disappeared or temporarily experience a short period of data loss. Thus we may remove the track for the object only if it has failed to associate with any ROI within τ_d time steps since $t_1^{k'}$, the last time step the k'th track can be associated with a region. Let $p_d^{k'}$ be a measure of persistence that the k'th track cannot be associated with a region or a measurement in a given period as follows

$$p_d^{k'} = \frac{t - t_1^{k'}}{\tau_d}, \; k' = 1, ..., K_t^d. \tag{37}$$

The closer the value of $p_d^{k'}$ to 1, the more certain that the k'th track should be removed. Accordingly, we may select track k for track removal if $p_d^k \geq 1$, $k \in \{1, ..., K_t^d\}$, yielding $K_t = K_{t-1} - 1$ after the execution of the death move. The schema for the death move is summarised as follows.

Death Move

1. Follow the steps in Section 3 to identify K_t^d tracks that cannot be associated with any ROIs or measurements.
2. Compute the set of discrete persistence measures $p_d^{k'}$ in (37) for $k' \in \{1, ..., K_t^d\}$, and then execute the track removal as follows
 • If $p_d^k \geq 1$, $k \in \{1, ..., K_t^d\}$, then for $i \in \{1, ..., N\}$,
 – Remove track k and its corresponding particles from the tracker as follows

$$\boldsymbol{x}_t^{(i)} = [\boldsymbol{x}_{1,t-1}^{(i)T}, ..., \boldsymbol{x}_{k-1,t-1}^{(i)T}, \boldsymbol{x}_{k+1,t-1}^{(i)T} ..., \boldsymbol{x}_{K_{t-1}^{(i)},t-1}^{(i)T}]^T.$$

 – Decrement the number of targets by one, i.e., $K_t^{(i)} = K_{t-1}^{(i)} - 1$.
 • else, goto Step 3
3. Perform target state estimation with the updated particles $\{\boldsymbol{x}_t^{(i)}, K_t^{(i)}\}_{i=1}^N$ using the update move in Section 4.

Update Move

In the update move, we only need to update the target states with a common value of number of targets $K_t^{(i)} = K_{t-1}^{(i)}$, using the sequential importance sampling method in Section 4. The schema for the update move is summarised as follows.

Update Move

1. Draw samples $\boldsymbol{x}_t \sim q(\boldsymbol{x}_t | \boldsymbol{x}_{t-1}^{(i)}, K_t^{(i)}, K_{t-1}^{(i)}, \boldsymbol{\mathcal{Y}}_t)$ in (35).
2. For each particle $\boldsymbol{x}_t^{(i)}$, compute the $\mathfrak{M}_t^{(i)}$-best solutions $\{\boldsymbol{\alpha}_t^l\}_{l=1}^{\mathfrak{M}_t^{(i)}}$ with the current observation $\boldsymbol{y}_t$ using the 2-D assignment algorithm, and then construct a discrete proposal function with the corresponding utility values to sample $\boldsymbol{\alpha}_t^{(i)}$ as in (33).
3. Compute the importance weight $w_t^{(i)}$ by substituting the particle $\{\boldsymbol{x}_t^{(i)}, K_t^{(i)}, \lambda_t^{(i)}\}$ in (34) for $i \in \{1, ..., N\}$.
4. Resample the particles if the effective sample size falls below a predefined threshold.

---

5. Clustering Algorithm

The general idea of the clustering algorithm is to group a collection of observations $\boldsymbol{\mathcal{Y}}_t = \{\boldsymbol{y}_{t'}\}_{t'=t-\tau}^t$, where τ is the size of a sliding window, that are in the spatial vicinity of each other at different time steps. If the targets, if present, are widely separated, the observations originating from these targets, in theory, are clustered in the locations where the targets have visited from $t - \tau$ to t. Using these clusters, or otherwise known as the ROIs, one may perform the target detection by monitoring the appearance and disappearance of the ROIs (see Section 3), and multi-target state estimation in the SMC framework by the data-dependent importance sampling (see Section 4).

Clustering algorithm

Given a set of independent observations $\boldsymbol{\mathcal{Y}}_t$, we would like to find a set of ROIs, $\boldsymbol{\mathcal{S}}_t = \{\mathcal{S}_t^{(j)}\}_{j=1}^{J_t}$, which are subspaces of $\mathcal{R}_V$, i.e., $\boldsymbol{\mathcal{S}}_t \subset \mathcal{R}_V$. The jth region $\mathcal{S}_t^{(j)}$ comprises $P_t^{(j)}$ measurements at successive scans in $\boldsymbol{\mathcal{Y}}_t$ that are believed to originate from the true targets. Denote the measurement difference between the mth and lth measurements of $\boldsymbol{y}_{t'+1}$ and $\boldsymbol{y}_{t'}$, i.e., $\boldsymbol{y}_{m,t'+1}$ and $\boldsymbol{y}_{l,t'}$, by $\boldsymbol{e}_{m,l}(t'+1, t') = \boldsymbol{y}_{m,t'+1} - \boldsymbol{y}_{l,t'}$, whose covariance matrix is, approximately, given by

$$\boldsymbol{\Sigma}_e \approx 2\boldsymbol{\Sigma}_w, \tag{38}$$

where we assume that the target that may have contributed the measurements $\boldsymbol{y}_{m,t'+1}$ and $\boldsymbol{y}_{l,t'}$ evolves slowly – in other words our covariance results will be approximate only. Denote the normalised distance by $d_{m,l}(t'+1, t')$ between $\boldsymbol{y}_{m,t'+1}$ and $\boldsymbol{y}_{l,t'}$ by

$$d_{m,l}(t'+1, t') = \boldsymbol{e}_{m,l}^T(t'+1, t') \boldsymbol{\Sigma}_e^{-1} \boldsymbol{e}_{m,l}(t'+1, t') \geq 0, \tag{39}$$

where $m \in \{1, ..., M_{t'+1}\}$ and $l \in \{1, ..., M_{t'}\}$. For all measurements of $\boldsymbol{y}_{t'+1}$, we have a set of normalised distances $\{d_{m,l}(t'+1, t')\}_{m=1}^{M_{t'+1}}$. Let $d_{m^*,l}(t'+1, t')$, $m^* \in \{1, M_{t'+1}\}$ be the minimum of this set. The measurements $\{\boldsymbol{y}_{m^*,t'+1}, \boldsymbol{y}_{l,t'}\}$ in terms of the time and observation indices $(t'+1, m_{t'+1}^*)$ and $(t', l_{t'})$ will be grouped in the same cluster $\mathcal{S}_t^{(j)}$ if

$$d_{m^*,l}(t'+1, t') \leq \epsilon_y, \tag{40}$$

where $\epsilon_y \geq 0$ is a threshold to be determined. In other words, if two measurements at successive scans are separated with a normalised distance less than ϵ_y, they will be grouped. In case none of the measurements of $\boldsymbol{y}_{t'+1}$ can be grouped with $\boldsymbol{y}_{l,t'}$, we skip $\boldsymbol{y}_{t'+1}$ and continue the search procedure using $\boldsymbol{y}_{t'+p}$, $1 < p \leq \tau$ until (40) is satisfied. On the other hand, if $\{\boldsymbol{y}_{m^*,t'+1}, \boldsymbol{y}_{l,t'}\}$ can be grouped, the clustering continues by attempting to group $\boldsymbol{y}_{m^*,t'+1}$ with other measurements in the remaining observations.

Assuming that $\boldsymbol{e}_{m,l}(t'+1,t')$ is approximately Gaussian, we may express the quantity $d_{m^*,l}(t'+1,t')$ as a chi-squared random variable [2], i.e., $d_{m^*,l}(t'+1,t') \sim \chi^2_n$, where n is the degrees of freedom. As a result, we may determine the threshold of the distance metric ϵ_y as follows

$$\mathbf{Pr}\{d_{m^*,l}(t'+1,t') \leq \epsilon_y\} = 1 - \beta, \tag{41}$$

where β is a small tail probability. For instance, given a level of confidence, say $1 - \beta = 0.95$, we may say that with 95% confidence, the pair $\{\boldsymbol{y}_{m^*,t'+1}, \boldsymbol{y}_{l,t'}\}$ should be grouped, if $d_{m^*,l}(t'+1,t') \leq \epsilon_y$ is satisfied.

Since the measurements in an observation may originate from true targets or from clutter, it is necessary to distinguish between the detected regions that are due to targets or clutter. Exploiting the differing characteristics of their models, as described in Section 2, we expect that given a set of observations in τ successive scans, it is more likely for the measurements originating from a true target to be located in the vicinity of each other than those from clutter. In other words, it is expected that the number of clustered measurements in a region due to a true target is larger than that due to clutter. Let $\tau_{\min}$ be the minimum number of clustered measurements in a region required to identify a target. Therefore, if $P_t^{(j)} \geq \tau_{\min}$, then the jth region is classified as originating from a target; otherwise, it is discarded. In this paper, we use the threshold $\tau_{\min} = P_D\,\tau$.

The steps for clustering target measurements are summarised in the following schema.

Clustering the measurements from successive observations

Given a set of τ observations $\{\boldsymbol{y}_{t'}\}_{t'=t-\tau}^{t}$:

1. Select a measurement $\boldsymbol{y}_a = \boldsymbol{y}_{l,t'}$, $l \in \{1, ..., M_t\}$ to search for the jth region $\mathcal{S}_t^{(j)}$, $j \leq J_t$.
2. Group $\boldsymbol{y}_a$ with $\boldsymbol{y}_b = \boldsymbol{y}_{m,t'+1}$, for all $m \in \{1, ..., M_{t'+1}\}$ according to (39).
 - If (40) is satisfied,
 – then, group $\{\boldsymbol{y}_a, \boldsymbol{y}_b\} \rightarrow \mathcal{S}_t^{(j)}$ in the same cluster and replace $\boldsymbol{y_a} = \boldsymbol{y}_{m^*,t'+1}$.
 – else, keep $\boldsymbol{y}_a$ intact and skip the observation $\boldsymbol{y}_{t'+1}$.
 - Goto step 2 with $t' \leftarrow t'+1$.
3. When all τ observations have been visited,
 - a region $\mathcal{S}_t^{(j)}$ is formed, only if $P_t^{(j)} \geq \tau_{\min}$.
 - goto step 1 with $l \leftarrow l+1$.
4. A set of target regions $\boldsymbol{\mathcal{S}}_t = \{\mathcal{S}_t^{(j)}\}_{j=1}^{J_t}$ has been found.

In the case where P_D is low in which data loss could occur, we may combine the search results from several windows, say τ_0. That is, the buffer contains observations $\boldsymbol{\mathcal{Y}}_t = \{\boldsymbol{y}_{t'}\}_{t'=t-\tau_0-\tau}^{t}$, and the clustering algorithm groups the measurements within a sliding window with size τ and repeats the search for τ_0 times by shifting the window by one time step at a time. While this search routine may seem redundant, it is robust to data loss in clustering the measurements originating from the same target or event. It also provides more reliable search results for target regions, because a true target is more likely to be detected by more than one window.

Target state initialisation for new track initiation—Given a set of ROIs, we can now systematically initialise the target state vector of a new track after a new target has been detected. We may draw samples within the subspaces of $\mathcal{R}_V$, i.e., $\mathcal{S}_t^{(j)}$, $j \in \mathcal{I}_b$, where each region represents *when and where* a new event is persistently happening. Hence, this proposed target initialisation is more effective and efficient, for it is likely that the particles drawn around these ROIs are better candidates to approximate the true distribution of the target states.

Before we present the initialisation of particles, we first rearrange the state vector $\boldsymbol{x}_{k,t} = [x_{k,t}, \dot{x}_{k,t}, y_{k,t}, \dot{y}_{k,t}]^T$ in the following form

$$\tilde{\boldsymbol{x}}_{k,t} = \begin{bmatrix} \boldsymbol{u}_{k,t} \\ \dot{\boldsymbol{u}}_{k,t} \end{bmatrix}, \; \boldsymbol{u}_{k,t} = \begin{bmatrix} x_{k,t} \\ y_{k,t} \end{bmatrix}, \; \dot{\boldsymbol{u}}_{k,t} = \begin{bmatrix} \dot{x}_{k,t} \\ \dot{y}_{k,t} \end{bmatrix}, \tag{42}$$

where $\boldsymbol{u}_{k,t}$ and $\dot{\boldsymbol{u}}_{k,t}$ are the xy position and velocity of the kth target, respectively. Here we propose to initialise $\boldsymbol{u}_{k,t}$ and $\dot{\boldsymbol{u}}_{k,t}$ separately, and then rearrange the initialised elements back into $\boldsymbol{x}_{k,t}$. We first denote the maximum and minimum velocities of all targets by $v_{\min}$ and $v_{\max}$, respectively. These bounds represent prior information about the physical limitations of the targets to be tracked. Let $t = t_0$ be the time when the kth track is initiated, and $\mathcal{S}_{t_0}^{(j)}$ be the ROI associated with the kth track. Then we sample $\dot{\boldsymbol{u}}_{k,t_0}$ for $i = \{1, ..., N\}$ uniformly as follows

$$\dot{\boldsymbol{u}}_{k,t_0}^{(i)} \sim p(\dot{\boldsymbol{u}}_{k,t_0} | v_{\min}, v_{\max}) = \mathcal{U}_{[v_{\min}, v_{\max}]^2}, \tag{43}$$

which is the initial velocity prior for a target.

Given that the detected regions are in the observation space, to sample the xy positions given $\mathcal{S}_{t_0}^{(j)}$, we need to define an inverse mapping $\boldsymbol{h}(\cdot) = \boldsymbol{g}^{-1}(\cdot)$ that *uniquely* converts the observation space into the xy-space, $\mathcal{R}_U$, where $\boldsymbol{g}(\cdot)$ is defined in (6), i.e., $\mathcal{R}_U = \boldsymbol{h}(\mathcal{R}_V)$. Assume the prior distribution of target xy position $p(\boldsymbol{u}_{k,t_0} | \mathcal{R}_U)$ to be

$$p(\boldsymbol{u}_{k,t_0} | \mathcal{R}_U) = \mathcal{U}_{\mathcal{R}_U}(\boldsymbol{u}_{k,t_0}), \tag{44}$$

i.e., the target initial xy positions are distributed uniformly in the state-space $\mathcal{R}_U$. We denote the ROI in the state-space by $\mathcal{Z}_{k,t_0} = \boldsymbol{h}(\mathcal{S}_{t_0}^{(j)})$, such that we propose to draw the samples of $\boldsymbol{u}_{k,t}$ for $i = \{1, ..., N\}$ uniformly as follows

$$\boldsymbol{u}_{k,t_0}^{(i)} \sim q(\boldsymbol{u}_{k,t_0}|\mathcal{Z}_{k,t_0}) = \mathcal{U}_{\mathcal{Z}_{k,t_0}}(\boldsymbol{u}_{k,t_0}). \quad (45)$$

6. $\mathfrak{M}$-BEST 2-D MEASUREMENT-TO-TARGET ASSIGNMENT ALGORITHM

The 2-D assignment algorithm [19], [26] is an intuitive method for solving classical assignment problems, which includes the data association problem for MTT applications, given that the assignment is always on a one-to-one basis. This approach globally searches for the *best* feasible solution that minimises a 2-D cost function, subject to a set of constraints. This efficient approach performs very well when compared to other data association methods, especially when the targets are widely separated. However, when the targets are closely spaced, the best solution approach may not provide reliable performance, leading to track loss and improperly partitioned measurements into tracks and false alarms. To mitigate the drawback inherited from the hard irrevocable decisions provided by the best-solution approaches, it is suggested [19], [26] that the $\mathfrak{M}$-best assignment algorithm be used that provides a set of feasible solutions with their own probabilities. It becomes more flexible to deal with the data association problem with this set of feasible solutions.

The measurement-to-target assignment problem can be cast as a constrained optimisation problem [19], [26] that maximises a function $C(\cdot)$ as follows

$$\boldsymbol{A}_t^j = \arg \max_{\boldsymbol{A}_t \in \boldsymbol{\mathcal{A}}^j} \left\{ C(\boldsymbol{\alpha}_t, \boldsymbol{x}_t, \boldsymbol{y}_t) \right\}, \quad (46)$$

where $\boldsymbol{A}_t^j$, which is the jth best solution in the feasible solution space $\boldsymbol{\mathcal{A}}^j$, can be easily mapped to $\boldsymbol{\alpha}_t$, subject to

$$\sum_{k=0}^{K} a_{l,k}^j = 1, \quad l \in \{1, ..., M_t\}, \quad (47)$$

$$\sum_{l=1}^{M_t} a_{l,k}^j = 1, \quad k \in \{1, ..., K\}, \quad (48)$$

$$\boldsymbol{\mathcal{A}}^j \in \boldsymbol{\mathcal{A}} - \bigcup_{p=1}^{j-1} \boldsymbol{A}_t^p, \quad (49)$$

where $\boldsymbol{\mathcal{A}}$ is the space for *all* feasible assignments. The binary assignment variable $a_{l,k}^j$, the l, kth elemement of $\boldsymbol{A}_t^j$, indicates whether the l, kth indices should be taken in the solution. If $a_{l,k}^j = 1$, then $\alpha_{l,t}^j = k$; otherwise $\alpha_{l,t}^j = 0$. The l, kth element of $C(\boldsymbol{\alpha}_t, \boldsymbol{x}_t, \boldsymbol{y}_t)$, which is the probability of assigning measurement $\boldsymbol{y}_{l,t}$ to target k, is given by

$$c_{l,k} = \begin{cases} 0, & \text{if } k = 0, \\ \log \left\{ \frac{P_D\, p(\boldsymbol{y}_{l,t}|\boldsymbol{x}_t, \alpha_l = k)}{p(\boldsymbol{y}_{l,t}|\alpha_l = 0)} \right\}, & \text{if } \log(\cdot) > 0, \\ -\infty, & \text{otherwise,} \end{cases} \quad (50)$$

for $l \in \{1, ..., M_t\}$ and $k \in \{1, ..., K_t\}$. Accordingly, this problem can be reformulated [19], [26], subject to the constraints (47) to (49), as

$$\boldsymbol{A}_t^j = \arg\max \sum_{k=0}^{K} \sum_{l=1}^{M_t} c_{l,k}\ a_{l,k}^j. \quad (51)$$

Details of how this algorithm works can be found in [19], [26].

Given the set of $\mathfrak{M}_t$-best solutions and their associated probabilities $\{u(\boldsymbol{\alpha}_t^j)\}_{j=1}^{\mathfrak{M}_t}$, where

$$u(\boldsymbol{\alpha}_t^j) \propto \exp(\sum_{l,k \in \boldsymbol{a}_t^j} c_{l,k}), \quad \sum_{j=1}^{\mathfrak{M}_t} u(\boldsymbol{\alpha}_t^j) = 1, \quad (52)$$

one can form the point-mass probability distribution function for $\boldsymbol{\alpha}_t$ from which an association vector $\boldsymbol{\alpha}_t$, with associated probability $u(\boldsymbol{\alpha}_t)$, can be sampled, i.e.,

$$\boldsymbol{\alpha}_t \sim q(\boldsymbol{\alpha}_t|\boldsymbol{x}_t, \boldsymbol{y}_t) \propto \sum_{j=1}^{\mathfrak{M}_t} u(\boldsymbol{\alpha}_t^j)\delta(\boldsymbol{\alpha}_t - \boldsymbol{\alpha}_t^j). \quad (53)$$

Note that in practice the value of $\mathfrak{M}_t$ can be determined by checking whether $u(\boldsymbol{\alpha}_t^m)$ is significant when compared with the culmulative probability $\sum_{j=1}^{\mathfrak{M}_t} u(\boldsymbol{\alpha}_t^j)$. For example, the $\mathfrak{M}_t$th solution is included if

$$\frac{u(\boldsymbol{\alpha}_t^{\mathfrak{M}_t})}{\sum_{j=1}^{\mathfrak{M}_t} u(\boldsymbol{\alpha}_t^j)} \geq 0.01. \quad (54)$$

7. COMPUTER SIMULATIONS

In this section, we examine the performance of the proposed algorithm with different experiments in the following areas: target detection, tracking, and data association, using a single sensor, located at $(x_o, y_o) = (0, 0)$. The environment in these experiments is very hostile in which the target detection probability $P_D = 0.5$ and the clutter density is $\Lambda_C \geq 10$. The surveillance region $\mathcal{R}_V$ is [2000, 2000]^2. The parameters for synthesising the scenarios in these experiements can be found in Table 7.1.

All targets are systhesised using a near constant velocity dynamic model [1], where the evolution of the kth targets in (1) is given by

$$\begin{aligned} \boldsymbol{x}_{k,t} &= \boldsymbol{A}_t \boldsymbol{x}_{k,t-1} + \boldsymbol{B}_t \boldsymbol{v}_{k,t}, \\ &= [x_{k,t}, \dot{x}_{k,t}, y_{k,t}, \dot{y}_{k,t}]^T \end{aligned} \quad (55)$$

where $(x_{k,t}, y_{k,t})$ and $(\dot{x}_{k,t}, \dot{y}_{k,t})$ are the xy position and velocity of the kth target at time t. The matrices $\boldsymbol{A}_t$ and $\boldsymbol{B}_t$ are, repectively, given as follows

$$\boldsymbol{A}_t = \begin{bmatrix} 1 & T_s & 0 & 0 \\ 0 & 1 & 0 & 0 \\ 0 & 0 & 1 & T_s \\ 0 & 0 & 0 & 1 \end{bmatrix} \text{ and } \boldsymbol{B}_t = \begin{bmatrix} T_s^2/2 & 0 \\ T_s & 0 \\ 0 & T_s^2/2 \\ 0 & T_s \end{bmatrix}, \quad (56)$$

Parameters	Values
(x_o, y_o)	$(0, 0)$
$\mathcal{R}_V$	$[2000, 2000]^2$
σ_x^2, σ_y^2	5×10^{-4}
$\sigma_\theta^2, \sigma_r^2$	$[0.0001, 25]^T$
T_s	1
T	1000
τ, τ_0	5, 5
ϵ_y	1.96
τ_b, τ_d	$\tau, (\tau + \tau_0)/P_D$
μ	0.5

Table 7.1. Parameters for computer simulation.

where T_s is the sampling instant. All targets share this same dynamic model in these experiments. Moreover, the observation model we adopt is a nonlinear model and contains two components – bearing and range. The mth measurement of $\boldsymbol{y}_t$ is defined as follows

$$\boldsymbol{y}_{m,t} = \left[\begin{array}{c} \tan^{-1}\left(\frac{y_{k_t} - y_o}{x_{k,t} - x_o}\right) \\ \sqrt{(x_{k,t} - x_o)^2 + (y_{k_t} - y_o)^2} \end{array} \right] + \boldsymbol{w}_{m,t}. \tag{57}$$

The noises $\boldsymbol{v}_{k,t}$ and $\boldsymbol{w}_{m,t}$ are both white Gaussian random variables with their covariance matrices $\boldsymbol{\Sigma}_v$ and $\boldsymbol{\Sigma}_w$, resepectively, defined as

$$\boldsymbol{\Sigma}_v = \left[\begin{array}{cc} \sigma_x^2 & 0 \\ 0 & \sigma_y^2 \end{array} \right], \text{ and } \boldsymbol{\Sigma}_w = \left[\begin{array}{cc} \sigma_\theta^2 & 0 \\ 0 & \sigma_r^2 \end{array} \right]. \tag{58}$$

Experiment 1: Joint target detection and tracking for multiple targets

In this experiment, we will consider $K_o = 4$ targets which evolve independently according to the constant velocity model, appear and disappear at different times (see Table 7.2), and cross each other. They essentially evolve at the lower-right quadrant of Figure 1, which plots all the observations in this experiment. The environment is very hostile with $\Lambda_C = 10$ and $P_D = 0.5$. The parameters needed to perform the clustering algorithm, namely τ and τ_0 as described in Section 5, and those needed to perform the target detection, namely τ_b and τ_d as described in Section 3, are given in Table 7.1. A total of $N = 200$ particles is used in the particle filter for target tracking.

Figures 2–4 show the results of the joint target detection and tracking. According to Figure 2, except some delays incurred when new tracks are initiated and vanishing tracks are removed as described in Section 3, all targets are well detected and monitored. Table 7.2 compares the true number of targets and its estimate throughout the experiment. According to Table 7.2, one may realise that the proposed algorithm performs very well in target detection even though the environment is hostile. The delays experienced

Targets	True time intervals	Detected time intervals
1	$[219, 357]$	$[227, 377(361)]$
2	$[299, 463]$	$[308, 482(466)]$
3	$[149, 755]$	$[158, 772(756)]$
4	$[299, 661]$	$[299, 680(664)]$

Table 7.2. Times at which the true targets and their estimates appear and disappear for Experiment 1.

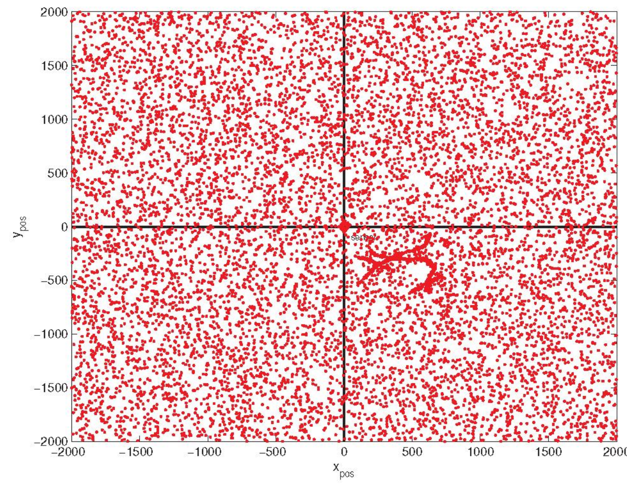

Figure 1. Synthesised observations within $\mathcal{R}_V = [-2,000, 2,000]^2$ with 4 targets, $P_D = 0.5$, and $\Lambda_C = 10$ for Experiment 1.

in the target detection are to avoid any premature initiation of new tracks and removal of existing tracks, based solely on the instantaneous number of detected ROIs. The values in the parenthesis in the detected time intervals in Table 7.2 are the times when the respective tracks were last associated with a ROI or a measurement. If a track cannot be associated with a ROI or a measurement for τ_d time steps, it will be removed.

Figure 3 shows all the ROIs found by the clustering algorithm in the absence of the observations. When comparing Figure 3 with Figure 1, we can say that the clustering algorithm performs very well in locating all the target originating events at the lower-right quadrant of both figures, while minimising the number of false alarms given the hugh clutter density Λ_C.

The tracking performance of the proposed algorithm is demonstrated in Figure 4. It is clear that all tracks follow the targets closely, and that those targets crossing each other are unambiguously resolved by the proposed data association approach. In particular, the track estimating Target 3 demonstrates the robustness of the data-dependent importance sampling method with the use of the ROIs representing this target. Unlike the other targets that evolve almost along a straight line, Target 3, which maneuvers with two

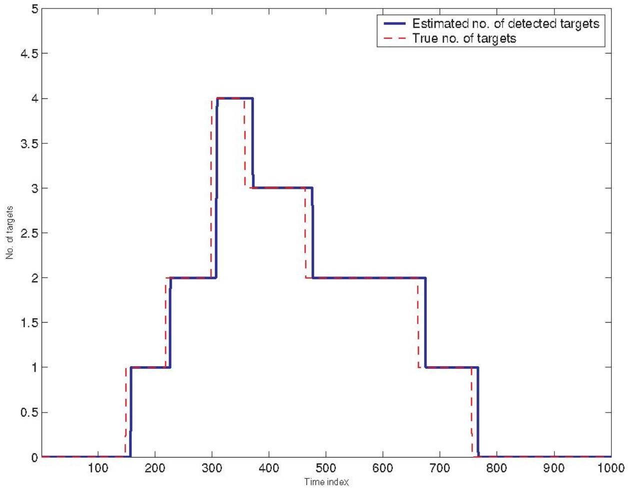

Figure 2. A comparison between the trajectories of the true number of targets and its estimate for Experiment 1.

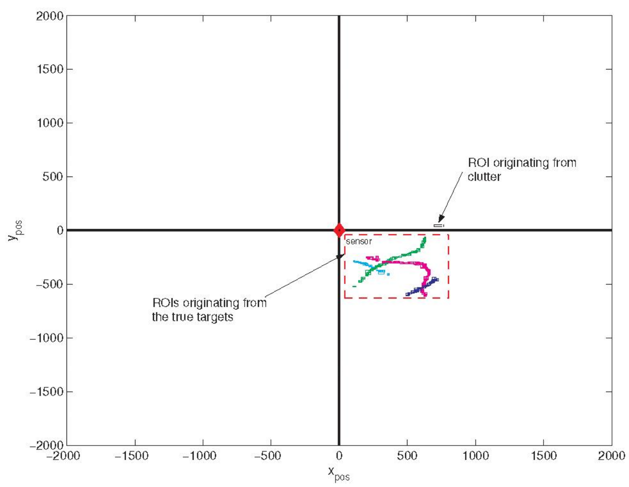

Figure 3. An illustration of all detected ROIs without the observations for Experiment 1.

sharp turns in its evolution, is well followed throughout its evolution, including the two sharp turns it makes. With the information from the ROIs, the tracker responds rapidly to the turns and provides representative particles to track these turns. Not only does the quick response demonstrated by the data-dependent importance sampling method enable better tracking performance, but it also reduces the possibility of track loss as a result of a model mismatch.

Here we evaluate the detection performance of the proposed method with different values of Λ_C for $P_D = 0.5$ and $K_o = 4$ targets. A total of 50 independent trials are run in the evaluation, and the results are shown in Figure 5, which demonstrates the robustness of the detection performance of the proposed algorithm even when $P_D = 0.5$ and $\Lambda_C = 20$ in correctly detecting the number of true targets as well as minimising the number of false tracks.

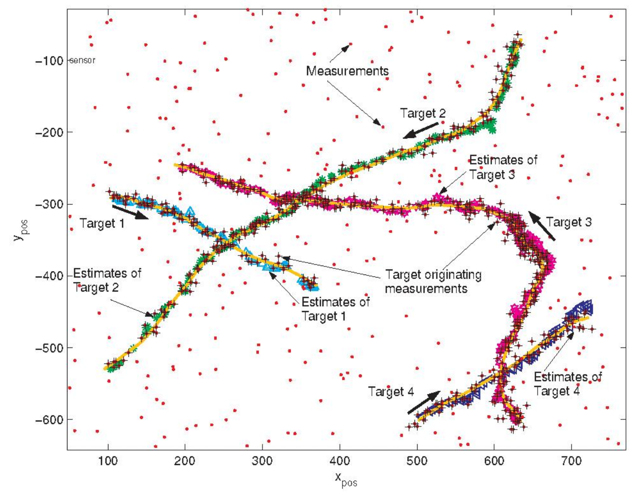

Figure 4. Synthesised tracks for $K = 4$ targets with $P_D = 0.5$, $\Lambda_C = 5$, $\mathcal{R}_V = [-2,000, 2,000]^2$: Crosses '+' represent the target originating measurements, dots '.' represent clutter measurements, solid lines represent true target trajectories, and other symbols represent target estimates for Experiment 1.

In addition, the tracking performances of the proposed method with the $\mathfrak{M}$-best solution approach, the auction, and the approach in [21] as a function of different numbers of particles $N = [100, 200, 500, 1000, 2000, 3000, 5000, 10000]$ are compared in terms of the Root Mean Square Error (RMSE), defined as

$$RMSE_l = \sqrt{\frac{1}{T}\sum_{t=1}^{T} ||\boldsymbol{x}_t - \hat{\boldsymbol{x}}_t^l(N)||^2 / K_t}, \qquad (59)$$

where $RMSE_l$ is the error for the lth independent run, and $\hat{\boldsymbol{x}}_t^l(N)$ is a posterior mean estimate of $\boldsymbol{x}_t$ for lth run with N particles. Here we provide the true value of K_t to the approaches for performance evaluation. For each value of N, a total of 20 independent runs were used with the same synthesised tracks with $P_D = 0.5$ and $\Lambda_C = 10$ but different observations, and the results are plotted in Figure 6. Each vertical line shown on the curve is the distribution of the the RMSE's for a particular value of N. As expected, for all approaches the RMSE decreases as N increases, at the expense of an increased computational load. According to Figure 6, as N is small, the 2-D assignment aproaches outperform the soft-gating approach, but as N is larger than 2000, the performance of the soft-gating approach is better than that of the auction approach and becomes comparable with that of the $\mathfrak{M}$-best approach.

Experiment 2: Comparison with the PHD filter

In this experiment, we intend to compare solely the target detection performance between the proposed method and the PHD filter [11], [12], [13], [14]. A scenario with a total of $K_o = 4$ targets appearing and disappearing at different

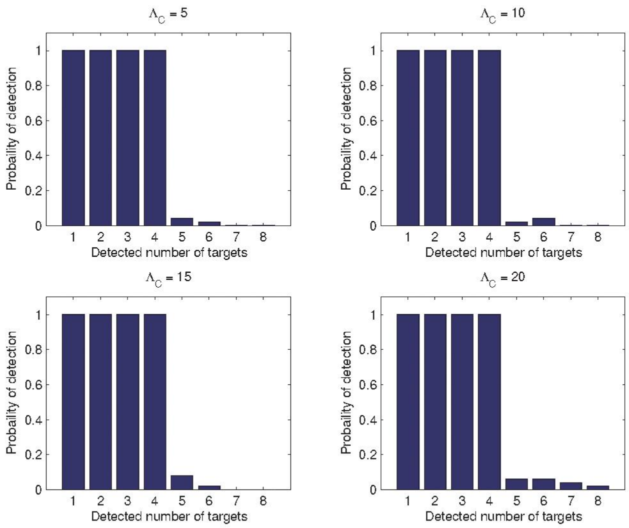

Figure 5. Evaluation of the proposed algorithm for target detection with $K_o = 4$ true targets for 50 independent trials in different environment for Experiment 1: $P_D = 0.5$ and $\Lambda_C = 5, 10, 15, 20$.

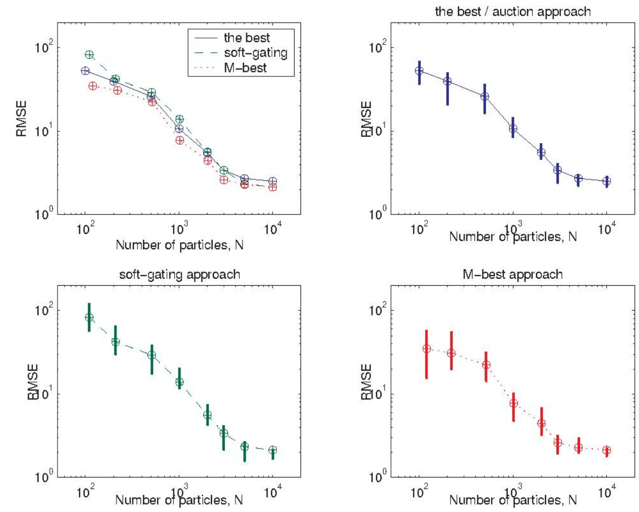

Figure 6. RMSE evaluated for different values of N for Experiment 1: 100, 200, 500, 1000, 2000, 3000, 5000, and 10000. Each vertical line on the curve represents the 1-σ error bars of the RMSE at a particular value of N.

times is synthesised with $P_D = 0.5$ and a set of clutter densities $\Lambda_C = [1, 3, 5, 10]$. For each value of clutter density, a total of 10 independent trials is run, and a total of $T = 500$ observations is generated for each trial.

When estimating the number of targets, $N_{PHD} = 2000$ particles are used for the PHD filter, whereas the number of particles $N = 100$ is fixed and used in the proposed method for all targets. Figures 7–10 summarise the results. It is found that the PHD estimates are noninteger and fluctuate around the true values. The higher the value of Λ_C, the more the estimates fluctuate, making the target detection by the PHD filter more ambiguous, as demonstrated in Figures 7(a)–10(a). Note that this ambiguity problem is even worse when one takes only one realisation for estimating the number of targets. For easier comparison, we compute the running average of the estimates using a sliding window with 5 samples at a time and then round the average up to the nearest integer, as shown in Figures 7(b)–10(b). When compared with the PHD filter, the proposed method is more robust and consistent to high clutter density, even though the number of targets is deterministically computed. Moreover, the performance of the PHD filter is very sensitive to the number of particles used, for a large number of particles is needed to explore the state-space for target detection. As a result, the computational intensity for the PHD is very high, which limits the practical value of the algorithm in online target detection. In contrast, the performance of the proposed method is not very sensitive to the number of particles used, and the detection is basically performed on the clustering of the observations and the association between the detected ROIs and the existing tracks. In comparison, not only is the proposed method more efficient and effective in detecting unknown and time-varying number of targets, it is also practical for real-time multitarget detection and tracking.

8. Conclusions

In this paper, we presented a hybrid approach for joint detection and tracking for multiple targets. In particular, we introduced a new deterministic clustering method to detect and monitor the appearance and disappearance of regions of interest (ROIs). These detected ROIs enable us to perform online target detection and draw better samples using the data-dependent importance sampling method in the context of sequential Monte Carlo framework. We also integrated an efficient and global data association method, given the latest observation and targets' state estimates, using the $\mathfrak{M}$-best 2-D data assignment algorithm with the sampling method. Computer simulations demonstrated that the proposed hybrid approach is very robust in detecting the ROIs originating from the true targets, even though the environment is very hostile in terms of high clutter density and low target detection probability, when compared with the PHD filter. Moreover, it was shown that the target tracking performance with the the $\mathfrak{M}$-best approach outperforms the other two approaches – the auction and the soft-gating.

9. Acknowledgements

The research of Ng, Li and Godsill was sponsored by the Data and Information Fusion - Defence Technology Centre, UK, Research Grant 10.2. Vermaak's work was funded by QinetiQ under contract QinetiQ Contract CU006 0000014890. The authors thank these parties for funding this work. Furthermore, the authors appreciate the valuable input from S. Maskell and M. Briers in QinetiQ, UK, for sharing the code of the auction algorithm for measurement-

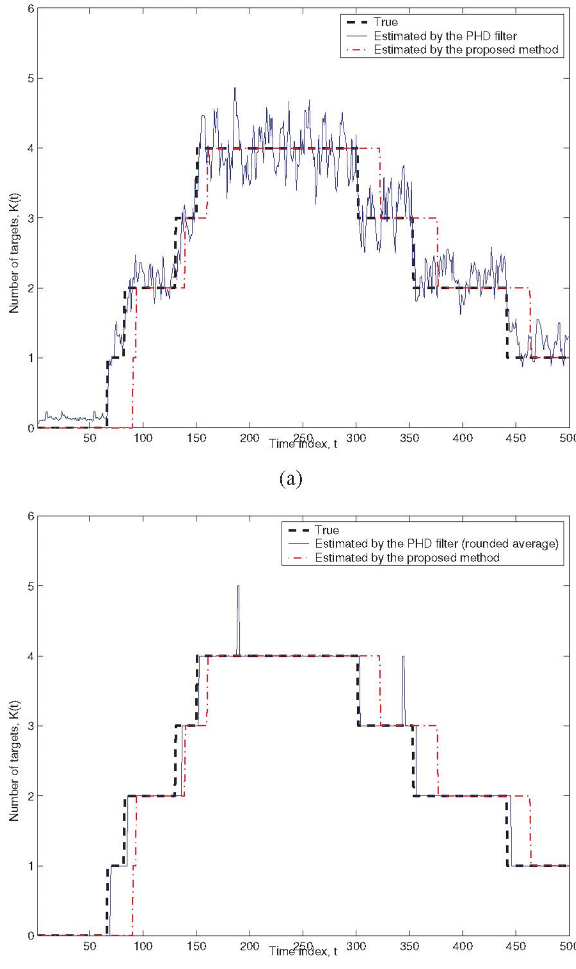

Figure 7. A comparison of the target detection performance between the proposed method and the PHD filter with $\Lambda_C = 1$ and $P_D = 0.5$.

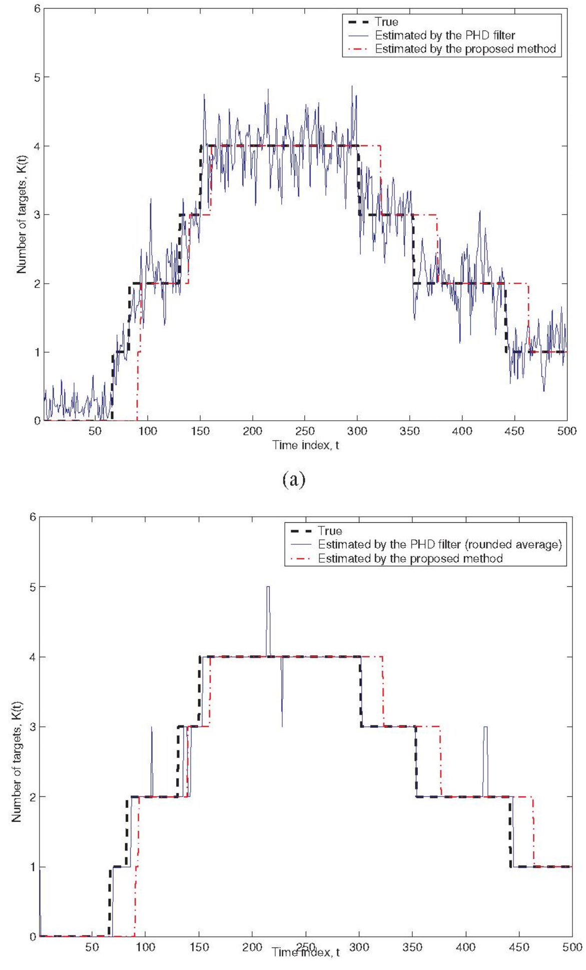

Figure 8. A comparison of the target detection performance between the proposed method and the PHD filter with $\Lambda_C = 3$ and $P_D = 0.5$.

to-target assignment.

REFERENCES

[1] Y. Bar-Shalom and T. E. Fortmann, *Tracking and Data Association*. Academic Press, 1988.

[2] X. R. Li, Y. Bar-Shalom, and T. Kirubarajan, *Estimation, Tracking and Navigation: Theory, Algorithms and Software*. New York: John Wiley & Sons, June, 2001.

[3] L. D. Stone, C. A. Barlow, and T. L. Corwin, *Bayesian Multiple Target Tracking*. Norwood, MA: Artech House, 1999.

[4] T. Fortmann, Y. Bar-Shalom, and M. Scheffe, "Sonar tracking of multiple targets using joint probabilistic data association," *IEEE Journal of Oceanic Engineering*, vol. 8, pp. 173–184, 1983.

[5] A. Doucet, N. de Freitas, and N. Gordon, eds., *Sequential Monte Carlo in Practice*. New York: Springer-Verlag, 2001.

[6] A. Doucet, S. Godsill, and C. Andrieu, "On sequential Monte Carlo sampling methods for Bayesian filtering," *Statistics and Computing*, vol. 10, pp. 197–208, 2000.

[7] J. Liu and R. Chen, "Sequential Monte Carlo Methods for Dynamic Systems," *Journal of the American Statistical Association*, vol. 93, no. 443, pp. 1032–1044, 1993.

[8] S. Haykin, *Adaptive Filter Theory*. Englewood Cliffs, NJ: Prentice Hall, 4th ed., 2000.

[9] N. Gordon, D. Salmond, and A. Smith, "Novel approach to non-linear/non-Gaussian Bayesian state estimation," *IEE Proceedings-F*, vol. 140, no. 2, pp. 107–113, 1993.

[10] G. Kitagawa, "Monte Carlo filter and smoother for

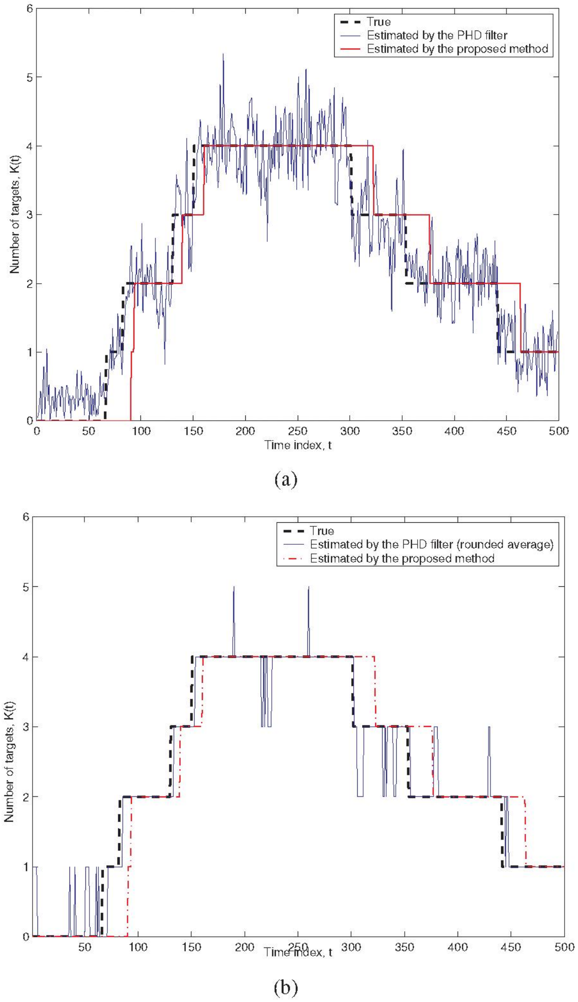

Figure 9. A comparison of the target detection performance between the proposed method and the PHD filter with $\Lambda_C = 5$ and $P_D = 0.5$.

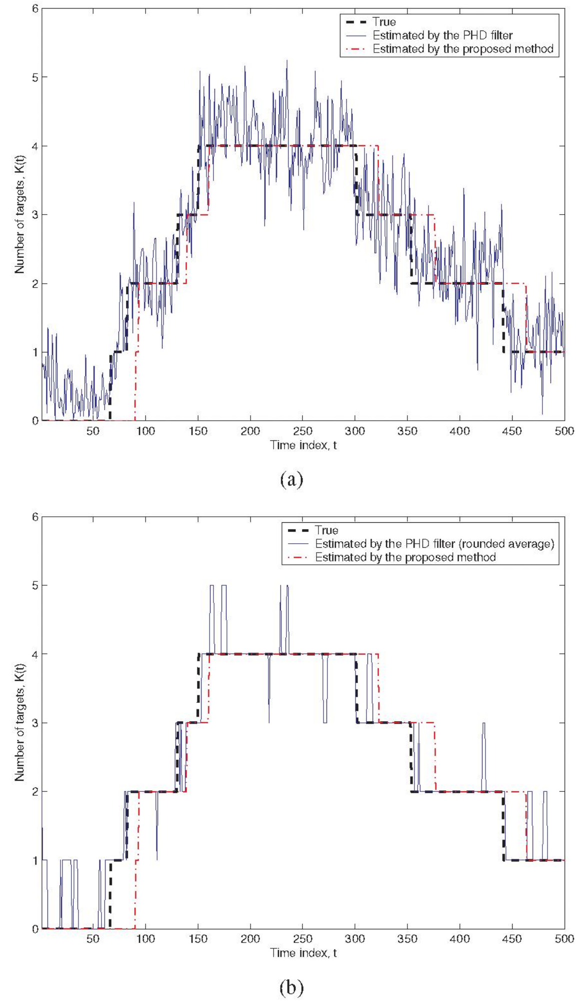

Figure 10. A comparison of the target detection performance between the proposed method and the PHD filter with $\Lambda_C = 10$ and $P_D = 0.5$.

non-Gaussian nonlinear state space models," *Journal of Computational and Graphical Statistics*, vol. 5, no. 1, pp. 1–25, 1996.

[11] H. Sidenbladh, "Multi-target particle filtering for the probability hypothesis density," *Proceedings 6th International Conference on Information Fusion*, pp. 800–806, 2003.

[12] H. Sidenbladh and S. L. Wirkander, "Particle filtering for finite random sets," *IEEE Transactions on Aerospace and Electronic Systems*, 2003. to appear.

[13] R. P. S. Mahler, "Multitarget Bayes filtering via first-order multitarget moments," *IEEE Transactions on Aerospace and Electronic Systems*, vol. 39, no. 4, 2003.

[14] B.-N. VO, S. Singh, and A. Doucet, "Sequential Monte Carlo implementation of the PHD filter for multi-target tracking," in *Proceedings of the International Conference on Information Fusion*, pp. 792–799, 2003.

[15] W. Ng, J. Li, S. Godsill, and J. Vermaak, "Multiple target tracking using sequential Monte Carlo methods and efficient data association and initialisation," *IEE Proceedings Radar, Sonar & Navigation*, 2004. Submitted to the IEE Proceedings Radar, Sonar & Navigation. See http://www-sigproc.eng.cam.ac.uk/ kfn20/.

[16] J. Larsen and I. Pedersen, "Experiments with the auction algorithm for the shortest path problem," *Nordic Journal of Computing*, vol. 6, no. 4, pp. 403–421, 1998.

[17] D. P. Bertsekas, "Auction algorithms for network flow problems: A tutorial introduction," *Computational Optimization and Applications*, vol. 1, pp. 7–66, 1992.

[18] R. D. Leone and D. Pretolani, "Auction algorithms for shortest hyperpath problems," *Society for Industrial and Applied Mathematics*, vol. 11, no. 1, pp. 149–159, 2001.

[19] S. Blackman and R. Popoli, *Design and Analysis of Modern Tracking Systems*. Norwood, MA: Artech House, 1999.

[20] M. S. Arulampalam, S. Maskell, N. Gordon, and T. Clapp, "A Tutorial on Particle Filters for Online Nonlinear/Non-Gaussian Bayesian Tracking," *IEEE Transactions on Signal Processing*, vol. 50, pp. 174–188, Feb. 2002.

[21] J. Vermaak, N. Ikoma, and S. J. Godsill, "Extended object tracking using particle techniques," in *Proceedings of the IEEE Aerospace Conference*, 2004.

[22] N. Ikoma and S. J. Godsill, "Extended object tracking with unknown association, missing observations, and clutter using particle filters," in *Proceedings of the 2003 IEEE Workshop on Statistical Signal Processing*, (St. Louis, MO), pp. 485–488, Sept. 2003.

[23] N. Gordon and A. Doucet, "Sequential Monte Carlo for maneuvring target tracking in clutter," in *Proceedings SPIE*, pp. 493–500, 1999.

[24] J. Bernardo and A. Smith, *Bayesian Theory*. New York: John Wiley & Sons, 1994.

[25] N. J. Gordon, D. J. Salmond, and D. Fisher, "Bayesian target tracking after group pattern distortion," in *Signal and Data Processing of Small Targets, SPIE 3163* (O. E. Drummond, ed.), pp. 238–248, 1997.

[26] Y. Bar-Shalom and W. D. Blair, *Multitarget-Multisensor Tracking: Applications and Advances*, vol. III. Norwood, MS: Archtech House, 2000.

William Ng *was born in Hong Kong. He received the B.Eng. degree from the University of Western Ontario, London, ON, in electrical engineering in 1994, the M.Eng. and Ph.D. degrees from McMaster Univeristy, Hamilton, ON, in 1996 and 2004, respectively, both in electrical engineering, and the M.M.Sc. from the Univeristy of Waterloo, Waterloo, ON, in management sciences in 2004. From 1996 to 1999, he was with Forschungszentrum Informatik, Karlsruhe, Germany, developing an expert system using neural networks for non-destructive pipeline evaluation, and from 1999 to 2002 he was with the Pressure Pipe Inspection Company Ltd., Missisauga, ON, where he was the head of Software and IT department. Currently, he is working in the Signal Processing Group at the Univeristy of Cambridge, Cambridge, U.K., as a research associate. His research interests include statistical signal processing for sensor arrays and multitarget tracking and multisource information fusion. Dr. Ng is a registered professional engineer in the province of Ontario since 2000. For more information see www-sigproc.eng.cam.ac.uk/~kfn20*

Jack Li, Junfeng *recieved the B.Eng. Degree from the University of Edinburgh, UK in electronic electrical engineeing in 2003. Currently, he is pursuing the P.h.D Degree in Statistical Signal Processing Group in the Information Engineering Division, Cambridge University Engineering Department. His research focuses on developing Sequential Monte Carlo (SMC) algorithms for dealing with Multsensor Multitarget tracking problems.*

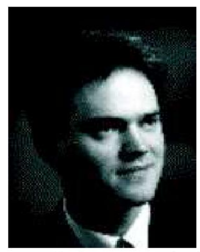

Simon Godsill *is Reader in Statistical Signal Processing in the Engineering Department of Cambridge University. He is an Associate Editor for IEEE Trans. Signal Processing and the journal Bayesian Analysis, and is a member of IEEE Signal Processing Theory and Methods Committee. He has research interests in Bayesian and statistical methods for signal processing, Monte Carlo algorithms for Bayesian problems, modelling and enhancement of audio and musical signals, source separation, tracking and genomic signal processing. He has published extensively in journals, books and conferences. He has co-edited in 2002 a special issue of IEEE Trans. Signal Processing on Monte Carlo Methods in Signal Processing and a recent special issue of the Journal of Applied Signal Processing, and organised many conference sessions on related themes.*

Jaco Vermaak *was born in South Africa in 1969. He received the B.Eng. and M.Eng. degrees from the University of Pretoria, South Africa in 1993 and 1996, respectively, and the Ph.D. degree at the University of Cambridge, U.K. in 2000. He has worked as a postdoctoral researcher at Microsoft Research Europe, Cambridge, U.K. between 2000 and 2002. He is currently employed as a senior research associate in the Signal Processing Group of the Cambridge University Engineering Department. His research interests include audio-visual tracking techniques, multi-media manipulation, statistical signal processing methods and machine learning.*